INL/MIS-23-73970-Revision-0

Fuel Flow Modeling under Thermal Fluidics Considerations within Operational Domains of Molten Salt Reactors

August 2023

Thabit M. A. Abuqudaira, Pavel V. Tsvetkov, Piyush Sabharwall

Changing the World's Energy Future

INL is a U.S. Department of Energy National Laboratory operated by Battelle Energy Alliance, LLC

INL/MIS-23-73970-Revision-0

Fuel Flow Modeling under Thermal Fluidics Considerations within Operational Domains of Molten Salt Reactors

Thabit M. A. Abuqudaira, Pavel V. Tsvetkov, Piyush Sabharwall

August 2023

Idaho National Laboratory
Idaho Falls, Idaho 83415

http://www.inl.gov

Prepared for the
U.S. Department of Energy
Under DOE Idaho Operations Office
Contract DE-AC07-05ID14517

Fuel Flow Modeling under Thermal Fluidics Considerations within Operational Domains of Molten Salt Reactors

Thabit M. Abuqudaira*, and Pavel V. Tsvetkov
Department of Nuclear Engineering, Texas A&M University
College Station, TX 77843, USA
*thabitne@tamu.edu; tsvetkov@tamu.edu

Piyush Sabharwall
Advanced Reactor Technology and Design, Nuclear Science & Technology, Idaho National Laboratory
Idaho Falls, ID 83415, USA
Piyush.Sabharwall@inl.gov

ABSTRACT

Molten Salt Reactors (MSRs) offer significant versatility supported by their design flexibility and safety advantages due to high temperatures, design customization capabilities, strong negative reactivity feedback effects, and salt chemistry characteristics. Different control schedules and different mass flow rates in the MSR primary systems impact neutronics and thermal hydraulics coupling. The result is two-fold. First, it leads to adaptability in various applications when the customization of a MSR unit is desired. Second, it calls for the quantification of dynamics and safety characteristics to assess the operational domain and make sure reactor stability and inherent safety characteristics are maintained. This paper provides an in-depth transient analysis of the operational implications of MSRs having heat-generating fuel and heat-transporting salt mixed forming liquid fuel salts contained within primary systems. A coupling model was developed to simulate fuel flow in molten salt reactors. A zero-dimensional reactor kinetics model was used with a one-dimensional heat transfer model in the reactor core. The temperature reactivity feedbacks of the fuel salt resulting from the thermal-hydraulics model were used in the reactor kinetics model to complete the coupled code. The model was first validated with the experimental results from the Molten Salt Reactor Experiment (MSRE). Then, it was applied to simulate the Molten Salt Breeder Reactor (MSBR) response at steady state and transients. The developed model was shown to be a suitable tool for the dynamic analysis of molten salt reactors.

KEYWORDS
Molten Salt Reactors, Fueled Salt, Reactor Operation, Fuel Flow, Transient Behavior

1. INTRODUCTION

In the United States, the interest in liquid fuel nuclear reactors has begun in the 1950s with the start of the Molten Salt Reactor Program (MSPR) at Oak Ridge National Laboratory (ORNL) [1]. In contrast to conventional nuclear reactors, a circulating liquid fuel salt is used in Molten Salt Reactors (MSRs) rather than regular solid fuel elements. Two demonstration MSRs were built and operated: the Aircraft Reactor Experiment (ARE) and the Molten Salt Reactor Experiment (MSRE) [2], [3]. The ARE was successfully operated for around 100 hours while the MSRE was for 4.5 years [4]. Nevertheless, no commercial deployment of this reactor type was achieved.

In the last two decades, the MSR was chosen to be one of six reactors proposed by the GEN IV International Forum for the next generation of nuclear reactors [5]. The existing contemporary design field, as offered by commercial MSR vendors, is surveyed to develop a set of reference design configurations representing emerging systems and their expected operational domains. In contrast to the operating experience with thermal-spectrum MSRE, current research is focused on fast-spectrum MSRs to be used as burners of transuranic waste from Light Water Reactors (LWRs) [6]. Currently, a Molten Salt Research Reactor (MSRR) is under construction on the campus of Abilene Christian University (ACU). It is expected that it will achieve criticality by 2025 [7]. The reactor will be used for research and training in the MSR environment. In addition to that, it will play a major role in the U.S. molten salt reactor development and deployment efforts.

In MSR's Research and Development (R&D) programs, attention is given to reactor stability focusing on primary system dynamics as well as evaluations of secondary systems including heat rejection needs and environmental interface options deployed under various environmental constraints. Explored operational domains include traditional electricity generation, process heat applications, nuclear battery autonomous operation, and integrated system configurations combining multiple energy products and operation options in a single MSR system.

Advancement in MSRs demonstration requires advancement in the physical instrumentation systems capable to work under the reactor's harsh environment. The instrumentation is required to reliably measure reactor parameters under extreme conditions of temperature and the corrosion environment. The information gained from this instrumentation can be used for reactor control [8]. These instrumentation include nuclear instrumentations required to monitor the neutron flux and reactor power, process instrumentations for temperature, pressure, and flow measurements of the coolant salt, radiation monitoring instrumentation, and some other special instrumentation for specific purposes [9]. The sensors and instrumentation groups of a nuclear reactor are shown in Figure 1.

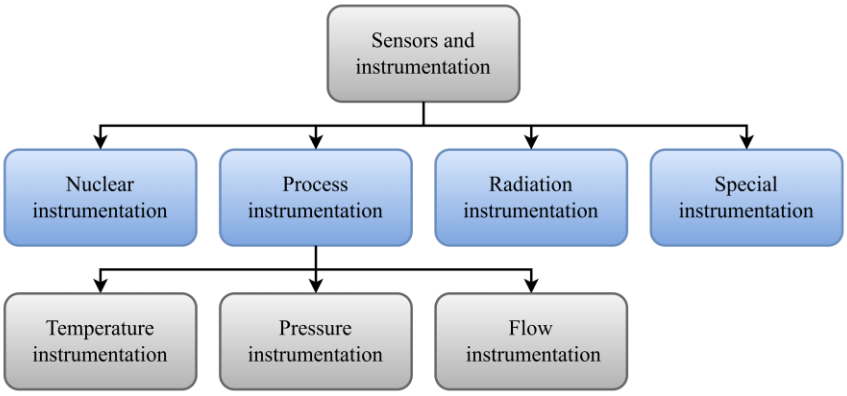

Figure 1. Instrumentation groups of a nuclear reactor.

Along with the physical instrumentation needs for the development of MSRs, parallel development in the computational codes accounting for the fuel salt movement is required. These computational tools will be used in parallel to the above-mentioned sensors and instrumentation. Neutronics and thermal-hydraulics coupling capabilities will play a significant role in the design and development of MSRs and other advanced nuclear reactors [10]. Based on the classification of neutronic solution methods (deterministic or Monte Carlo) and thermal-hydraulic solution methods (1, 2, or 3-Dimensional), various coupling strategies can be implemented. The research has been going to further develop MSRs modeling capabilities [11]–[14].

In this study, the fuel flow effects in MSRs on the heat transfer and the related reactivity feedbacks are investigated using the zero-dimensional reactor kinetics equation with one-dimensional heat transfer equations. A coupling neutronics thermal-hydraulics code was developed accounting for the fuel salt movement and the associated effects. The code is intended to be used for reactor dynamics and stability analysis studies for the MSRR that is under construction in the United States.

2. THE MOLTEN SALT BREEDER REACTOR

The Molten Salt Breeder Reactor (MSBR) is a conceptual design proposed by Oak Ridge National Laboratory (ORNL) [15]. It was proposed after the successful operation of the MSRE. The reactor was planned to be constructed and operated as a prototype reactor. The reactor is a 2250 MW_{th}, graphite-moderated, molten-salt-fueled reactor [16]. The molten salt fuel is pumped upward in the graphite-moderated reactor core to the tube side of the heat exchangers. In the heat exchangers, the heat is transferred to the secondary salt located in the shell side. The secondary salt is pumped to the steam generators completing a closed loop [17]. MSBR's basic flow diagram is shown in Figure 2.

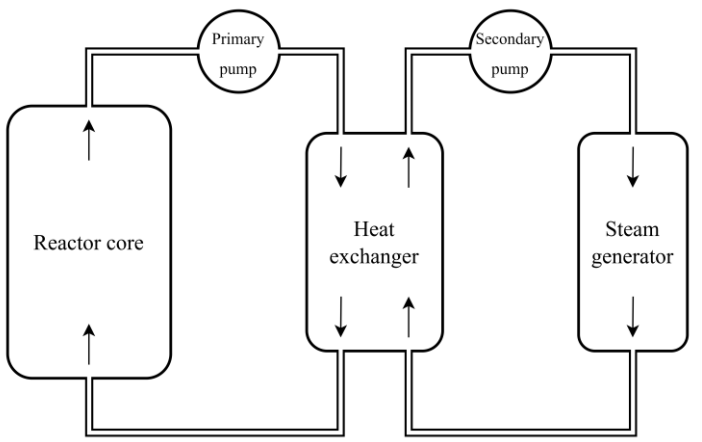

Figure 2. MSBR's basic flow diagram.

The fuel salt is a mixture of fluorides of lithium, beryllium, thorium, and uranium flowing through the core in a single pass. The fuel is composed of ^{233}U and ^{232}Th. The reactor core is composed of two zones. One central zone and one outer zone. Both have a height of 3.96 m. The reactor parameters are summarized in Table I [18]. The fuel salt transit time in various primary loop components and the heat and mass transfer parameters are summarized in Tables II and III.

Table I. MSBR summarized neutronics parameters.

Parameter	Symbol	Value	Unit
Reactor power	P	2250	MW_{th}
Mean neutron generation time	Λ	0.36	ms
Effective delayed neutron fraction	β_{eff}	0.00264	-
Effective delayed neutron decay constant	λ_{eff}	0.05	s^{-1}
Fuel salt temperature reactivity coefficient	α_f	-3.22	pcm/K
Graphite temperature reactivity coefficient	α_g	2.35	pcm/K
Fraction of fission energy released in the fuel	γ_f	0.97	-
Fraction of fission energy released in the graphite	γ_g	0.03	-

The fuel salt transit time will play a crucial role in determining the rate of precursors removal and addition to the reactor core. The total time during which the fuel salt will be out of the core is equal to the transit time in the hot leg, tube side of the heat exchanger, and cold leg.

Table II. Fuel salt transit time in the MSBR.

Parameter	Symbol	Value	Unit
Transit time in the core	τ_C	4.5	s
Transit time in the hot leg	τ_{HL}	2.1	s
Transit time in the heat exchanger	τ_H	1.8	s
Transit time in the cold leg	τ_{CL}	2.1	s
Transit time in the loop outside the core	τ_L	6	s

Table II. Heat and mass transfer parameters of the MSBR.

Parameter	Symbol	Value	Unit
Mass of the fuel salt in the core	m_f	54205	kg
Mass of the graphite in the core	m_g	122623	kg
Mass of the fuel salt in the heat exchanger	m_h	5384	kg
Specific heat capacity of the fuel salt	$c_{p,\,f}$	1357	J/kg.K
Specific heat capacity of the graphite	$c_{p,\,g}$	1758	J/kg.K
Total fuel to graphite heat transfer coefficient	$A \times h_{fg}$	24.8×10^6	W/K
Total fuel salt to the secondary salt heat transfer coefficient	$A \times h_{hc}$	19.8×10^6	W/K
Primary salt mass flow rate	$\dot{m}$	11944	kg/s

3. REACTOR MODELING

To study the fuel flow effects in flowing fuel cores, a neutronics thermal-hydraulic coupling code was developed using Visual Basic for Applications (VBA). The code uses the reactor parameters provided by ORNL. These parameters are used in the neutronics model to get the reactor power, net reactivity, and precursors population as a function of time. These parameters are then transferred to the thermal-hydraulics model where the axial temperature distribution in the reactor core is determined. The resulting temperatures will be used to provide the temperature reactivity feedbacks to the neutronics model completing a loop of coupled models. A scheme describing the coupling code is shown in Figure 3.

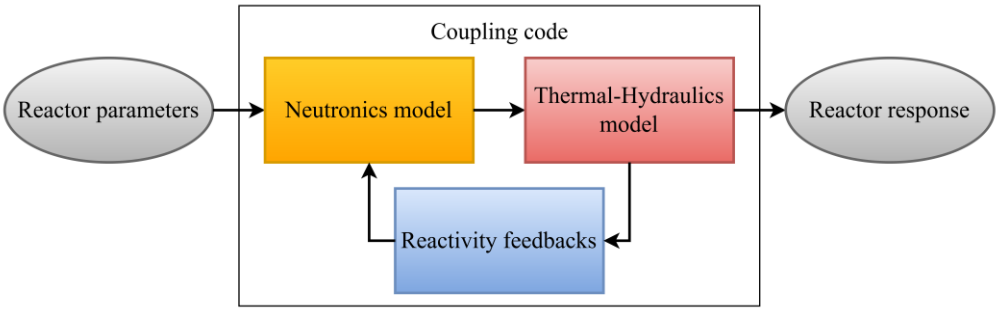

Figure 3. Overview of the developed coupling code scheme.

3.1. Neutronics Model

The reactor kinetics model was used to model the neutronic behavior of the reactor with one effective group of delayed neutrons. In the reactor kinetics, no spatial dependence is considered, that is, a zero-dimensional model of the reactor is used. The change in reactor power P(t) as a function of time can be described by:

$$\frac{dP(t)}{dt} = \frac{\rho_{net}(t) - \beta_{eff}}{\Lambda} P(t) + \lambda_{eff} C(t) \quad (1)$$

Where ρ_{net} is the net reactivity of the reactor core and C(t) is the precursors population in units of power as a function of time. The reactor net reactivity is equal to the summation of the steady-state reactivity, feedback reactivity, and any external reactivity. To account for the fuel salt movement, the conventional precursors population equation was modified by adding two terms accounting for the fuel salt removal and addition to the reactor core [19]:

$$\frac{dC(t)}{dt} = \frac{\beta_{eff}}{\Lambda} P(t) - \lambda_{eff} C(t) - \frac{1}{\tau_C} C(t) + \frac{e^{-\lambda_{eff} \tau_L}}{\tau_C} C(t - \tau_L) \quad (2)$$

At steady state, the non-zero steady-state reactivity of the core and the precursors population in the unit of power can be obtained from Equations 1 and 2.

3.2. Thermal-Hydraulics Model

In the thermal-hydraulics model, a nodal approach was used to account for the one-dimensional heat transfer in the primary circuit. The fuel salt and graphite in the reactor core and the fuel salt in the heat exchanger were divided into an equal number of nodes.

The effect of the number of nodes on the reactor parameters at steady state and following transients were studied. Overall, less deviation from the steady-state expected values was obtained using a greater number of nodes. However, a further increase in the number of nodes will increase the simulation time without significant improvement in the simulation accuracy. Fifteen axial nodes were adopted for the present study. The developed nodal approach is shown in Figure 4.

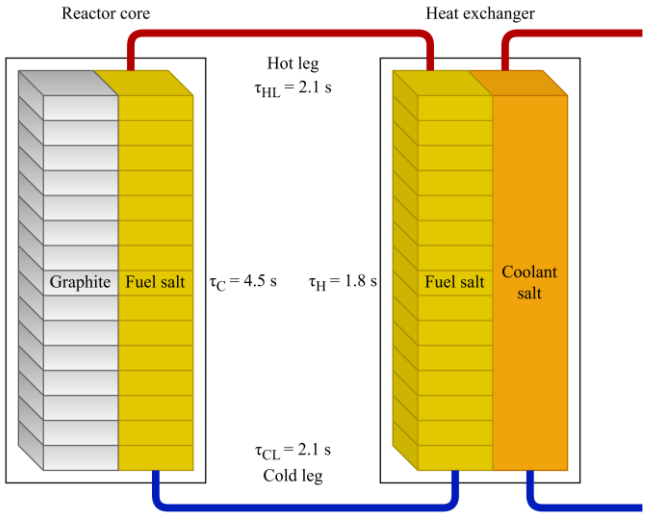

Figure 4. The developed nodal approach for MSBR.

In the heat transfer model, heat is generated in both the fuel salt and the graphite. The heat transfer equation for the fuel salt nodes in the reactor core is:

$$\frac{m_f}{N} c_{p,f} \frac{dT_{f,i}(t)}{dt} = \gamma_f f_i P(t) + h_{fg} \frac{A_{fg}}{N} \left[T_{g,i}(t) - T_{f,i}(t)\right] - \dot{m} c_{p,f} \left[T_{f,i}(t) - T_{f,i-1}(t)\right] \quad (3)$$

Where N is the number of nodes in the model, f_i is the fraction of power generated in the i^{th} node, h_{fg} is the fuel to graphite heat transfer coefficient, A_{fg} is the heat transfer area between the fuel and graphite, $T_{g,i}$ is the graphite temperature in the i^{th} node, $T_{f,i}$ is the fuel salt temperature in the i^{th} node.

For the first node, the term $T_{f,\,i-1}$ can be described in terms of the fuel salt temperature in the heat exchanger by knowing the fuel salt transit time in the cold leg:

$$T_{f,0}(t) = T_{h,N}(t - \tau_{CL}) \quad (4)$$

For the graphite nodes, the heat transfer equations were constructed in a similar way to the fuel salt in the reactor core equation:

$$\frac{m_g}{N} c_{p,\,g} \frac{dT_{g,\,i}(t)}{dt} = \gamma_g f_i P(t) - h_{fg} \frac{A_{fg}}{N} \left[T_{g,\,i}(t) - T_{f,\,i}(t)\right] \quad (5)$$

The temperature of the coolant salt in the shell side was assumed to be constant at 450 ℃ [20], [21]. For the fuel salt temperature in the heat exchanger, the heat transfer equation can be written as:

$$\frac{m_h}{N} c_{p,h} \frac{dT_{h,i}(t)}{dt} = \dot{m}_p c_{p,h} \left[T_{h,i}(t) - T_{h,i-1}(t)\right] - h_{hc} \frac{A_{hc}}{N} \left[T_{h,i}(t) - T_{c,i}(t)\right] \quad (6)$$

Where h_{hc} is the fuel salt to secondary salt heat transfer coefficient, A_{hc} is the heat transfer area between the fuel salt and the salt, and $T_{h,\,i}$ is the fuel salt temperature in the heat exchanger in the i^{th} node. Using the hot leg transit time, the first fuel salt node temperature in the heat exchanger can be described based on the fuel salt temperature in the reactor core:

$$T_{h,\,0}(t) = T_{f,\,N}(t - \tau_{HL}) \quad (7)$$

3.3. Coupling Code

The set of Ordinary Differential Equations (ODEs) resulting from the neutronics model and the thermal-hydraulics model were coupled numerically using Euler's method. Euler's method is a first-order numerical method used for solving ODEs. The effect of the time step on the accuracy was investigated. The usage of fine time steps showed less deviation from the steady-state expected values. However, a further decrease in the time step value will have no significant impact but increases the simulation time. An optimum time step of 1 ms was used in this study.

The reactor power was assumed to be uniformly generated in the axial direction. The feedback reactivity resulting from the fuel salt and graphite temperatures change in the reactor core was determined by:

$$\rho_{fb} = \alpha_f I_{f,i} \Delta T_{f,i} + \alpha_g I_{g,i} \Delta T_{g,i} \quad (8)$$

Where $I_{f,i}$ and $I_{g,i}$ are the neutron importance factors in the i^{th} node in the fuel and graphite moderator, respectively.

4. RESULTS AND DISCUSSION

The developed code was first validated with some of the available experimental data from the MSRE transient experiments. Then, the code was used to simulate the MSBR response at steady-state and due to transients.

4.1. Model Validation

The MSRE was a nuclear reactor experiment designed and operated by ORNL in the United States in the 1960s to demonstrate the feasibility of using liquid fuel in a nuclear reactor [22]. The reactor was operated with ^{235}U as the fissile material in the fuel salt mixture. Then ^{235}U was replaced by ^{233}U as the fissile material. The reactor operated at several power levels and reached a maximum power of about 8 MW_{th}. The MSRE experimental data generated during its operation helped to advance the understanding of the behavior of liquid fuels in nuclear reactors [23]. This experimental data is the only source of information from such a reactor environment.

In the present study, the MSRE with ^{233}U as the fissile material in the fuel salt mixture was used for the validation. Reactor geometry and the complete set of design parameters are obtained from ORNL reports and other published data [24], [25]. The same nodal approach developed for the MSBR was used for the MSRE with the exception that the MSRE contains an extra air loop connected to the coolant salt in the secondary loop. In addition to that, the MSRE has a negative graphite temperature reactivity coefficient while it is positive for the MSBR with the used parameters in this study.

The MSRE experimental data include the reactor power change following a transient caused by a step insertion of reactivity. Analysis of the experimental data showed that the MSRE has satisfactory inherent stability characteristics. The dynamic response of the reactor following a reactivity insertion at three different power levels was investigated and compared with ORNL experimental results [26]. A comparison of the developed code results with the experimental data is shown in Figures 5, 6, and 7.

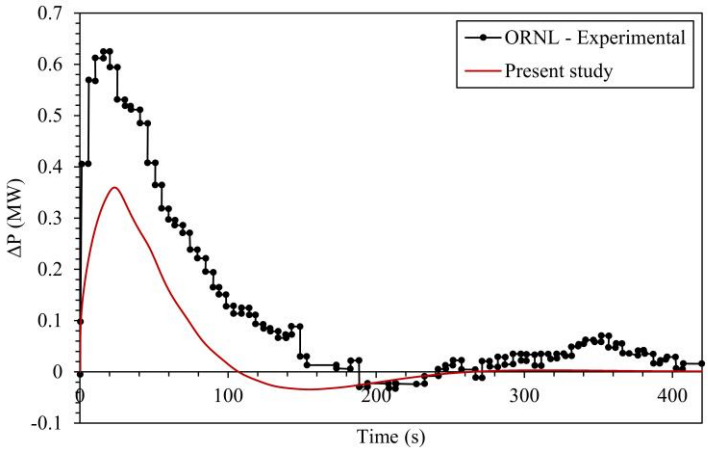

Figure 5. Reactor power change after step reactivity insertion of +13.9 pcm at 1 MW_{th}.

At the three power levels, the reactor power will promptly increase after the step reactivity insertion. This increase in reactor power will increase the fuel salt and graphite moderator temperatures and thus the temperature reactivity feedback will counteract this increase causing the power to decrease to its original

level. It was observed that the reactor power would return to its original power level more rapidly at higher power levels.

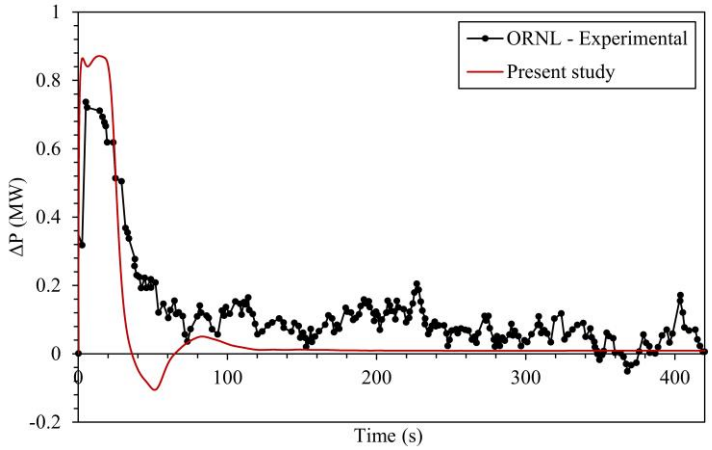

Figure 6. Reactor power change after step reactivity insertion of +19 pcm at 5 MW_{th}.

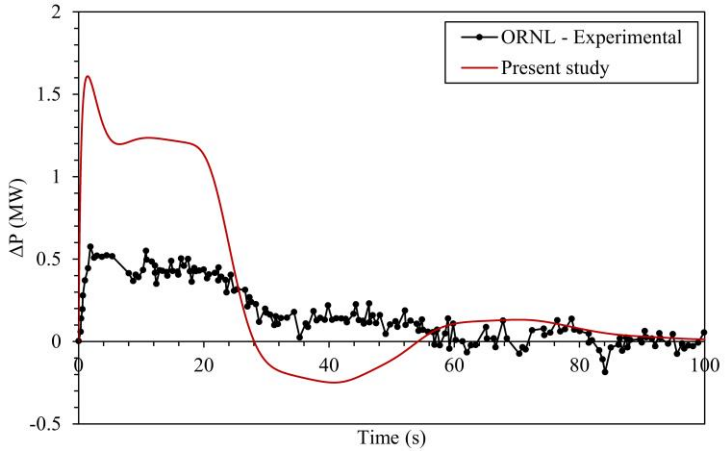

Figure 7. Reactor power change after step reactivity insertion of +24.8 pcm at 1 MW_{th}.

In comparison to the experimental results, the code overestimated the prompt increase in reactor power at 8 and 5 MW_{th} and underestimated it at 1 MW_{th}. However, it matched the experimental results in estimating the time step at which the power would return to its original value. This difference in the power peak following the reactivity insertion is mainly due to the usage of averaged heat transfer coefficients in the core (single region core) and other simplifications in the model. In addition to that, this deviation may be due to the inaccuracies in the provided reactor parameters. Several models using similar approaches had observed the same deviations in estimating the change in reactor power peak [27], [1].

It is expected to improve the simulated behavior by considering the radial power distribution in the core and fuel salt mixing effects, the usage of temperature-dependent heat transfer coefficients and neutron importance factors in each core node, and taking into account xenon concentration feedback. These modifications are under investigation. Overall, the present approach can be applied to other MSRs for dynamics and stability analysis studies.

4.2. MSBR Simulation

The developed code was used to simulate the MSBR response at steady-state and due to transients. The steady-state non-zero reactivity required to maintain criticality compensating for the reactivity loss due to fuel movement out of the core was determined. The reactor temperature distribution was obtained using the developed heat transfer equations. Axial steady-state temperature distribution in the MSBR primary circuit is shown in Figure 8. These calculated parameters were used as inputs to further investigate the code capabilities in simulating abnormal reactor conditions.

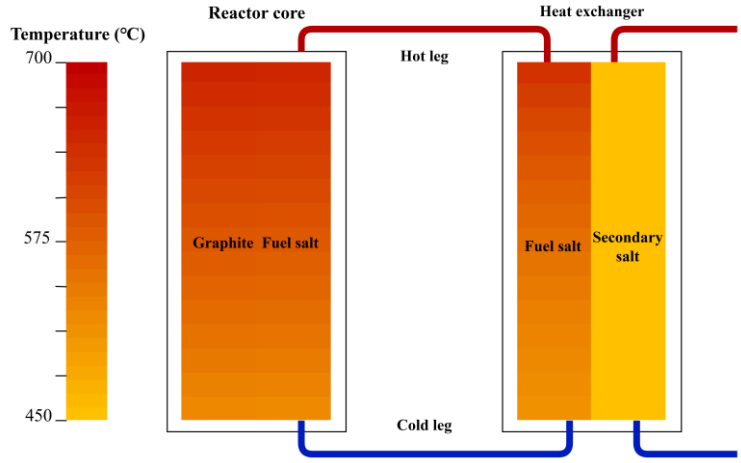

Figure 8. Axial temperature distribution in the primary circuit at steady state.

4.2.1. External reactivity insertion

In the proposed design of the MSBR, long-term reactivity control is performed by varying the fuel concentration in the fuel salt. Graphite control rods are used for power regulation during reactor operation. To simulate the effect of the control rods insertion and withdrawal, an external reactivity was inserted at t=0 in the model. The resulting reactor power as a function of time after an external reactivity insertion of $0.1\beta_{eff}$ is shown in Figure 9. The reactor power promptly increased with the reactivity insertion. The opposite was observed in the case of negative reactivity insertion of $0.1\beta_{eff}$. The negative fuel temperature reactivity coefficient counteracted the inserted reactivity and led to reactor power stabilization at a new lower level.

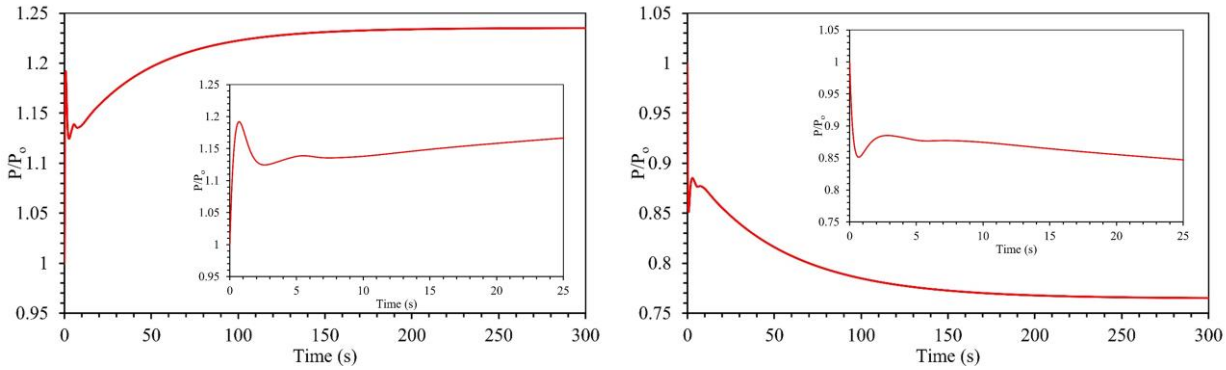

Figure 9. Reactor power after external reactivity addition. Left: $+0.1\beta_{eff}$, right: $-0.1\beta_{eff}$.

The fuel salt temperature in the reactor core and then in the heat exchanger followed the reactor power behavior. A slower response of the graphite temperature was observed. The change in the average temperature of the axial nodes is shown in Figure 10.

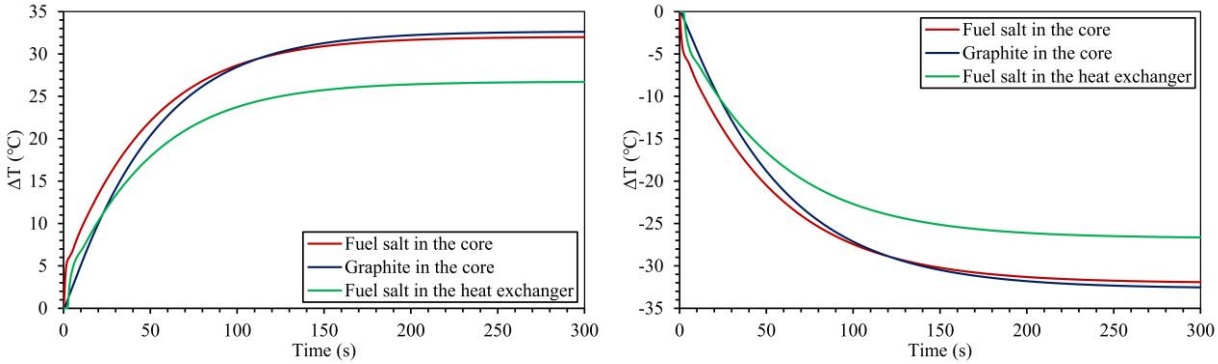

Figure 10. Average temperature change after external reactivity addition. Left: +0.1β_{eff}, right: -0.1β_{eff}.

4.2.2 Fuel flow transient

Different control schedules and different mass flow rates in the MSR primary systems impact neutronics and thermal hydraulics coupling. Quantification of dynamics and safety characteristics to assess the operational domain and make sure reactor stability and inherent safety characteristics are maintained is a crucial task. Variation of the primary circuit mass flow rate simulates the effect of the fuel salt concentration variation. Two transients simulating a change in the mass flow rate were conducted: increase by 10% and decrease by 10%. Reactor power change after the mass flow rate change is shown in Figure 11.

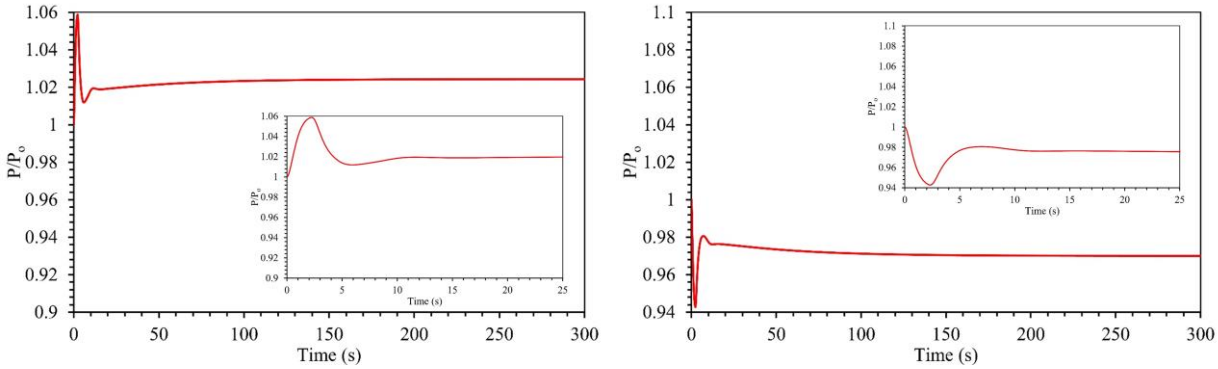

Figure 11. Reactor power after fuel salt mass flow rate transient. Left: + 10%, Right: -10%.

In comparison with the external reactivity insertion, the same behavior was achieved with the mass flow rate transient, that is: a prompt response was observed. The increase in the mass flow rate led to a prompt increase in the reactor power. This can be explained by the fact that the mass flow rate is directly proportional to the fuel salt concentration. However, the power change was lower in magnitude than in the reactivity insertion part. This can be explained by the fact that changing the flow of the fuel salt will change the rate of fuel and precursors removal and addition to the core.

The change in the average temperature of the axial nodes following the change in the mass flow rate is shown in Figure 12. It can be observed that the fuel salt temperature in the heat exchanger experienced a greater change in temperature following the transient. After a few seconds, the negative reactivity feedback stabilized the fuel salt temperature from further change.

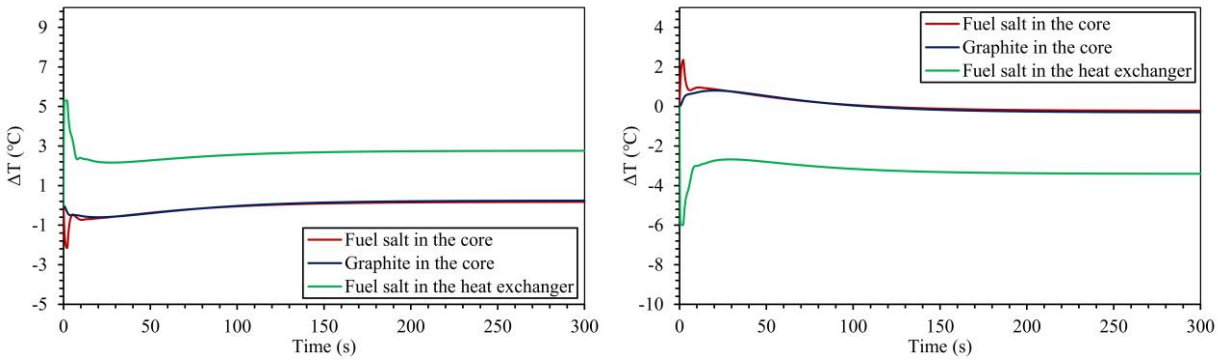

Figure 12. Average temperature change after fuel salt mass flow rate transient: Left – increase by 10% Right- decrease by 10%.

4.2.3. Heat sink transient

In the case where the secondary coolant (salt) temperature will change due to a transient, the reactor balance will be affected. The increase in the secondary coolant temperature will lead to a decrease in the rate of heat removal from the primary circuit. No power response was observed during the cold leg transit time. After this transit time, the reactor power started to decrease. The fuel salt temperature in the tube side of the heat exchanger rapidly increased. In contrast, the fuel salt temperature in the core started to increase after the fuel salt transit time in the cold leg. This increase in the temperature will lead to a counteracting reactivity feedback that will stabilize the reactor at a new power level. Reactor power and the average temperature change with time after the secondary coolant temperature increase by 10% are shown in Figures 13 and 14.

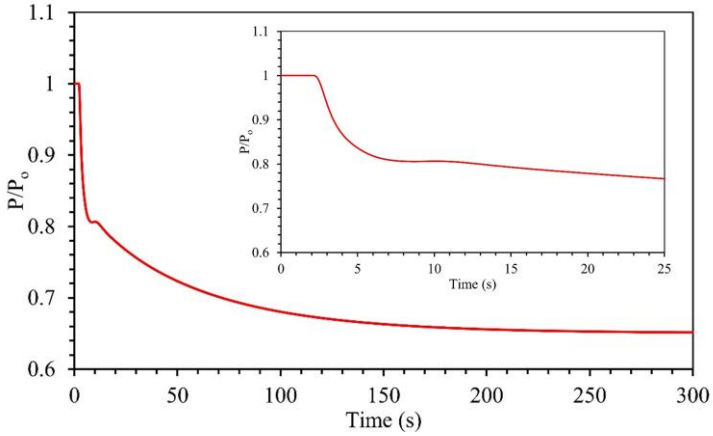

Figure 13. Reactor power after secondary coolant temperature increases by 10%.

The opposite will be observed in the case of a secondary coolant temperature decrease by 10%, the reactor power will increase after a time equal to the cold leg transit time. The reactor will stabilize at a

new power level because of the total negative reactivity feedback. The maximum temperature change is reached after the delay of the fuel salt in the cold leg. Reactor power and the average temperature change with time after the secondary coolant temperature decrease by 10% are shown in Figures 15 and 16.

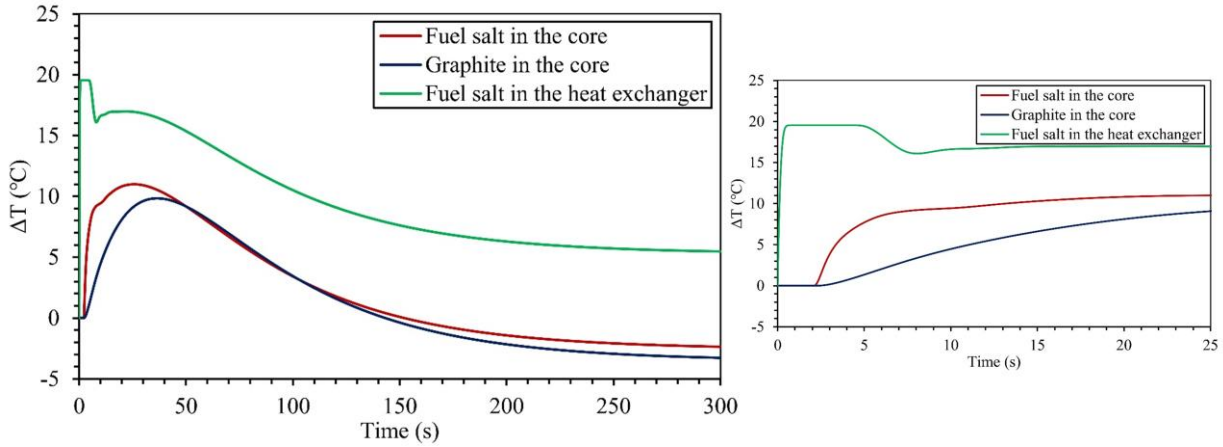

Figure 14. Average temperature change after secondary coolant temperature increases by 10%.

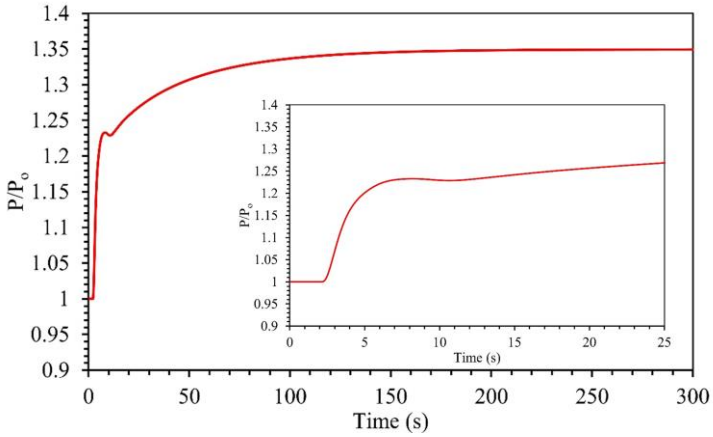

Figure 15. Reactor power ratio after the secondary coolant temperature decrease by 10%.

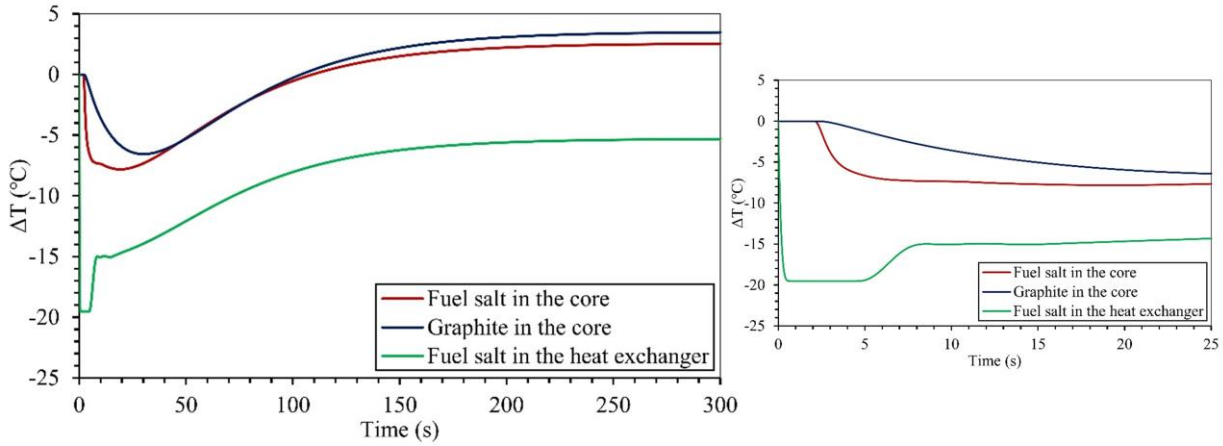

Figure 16. Average temperature change after secondary coolant temperature decrease by 10%.

5. CONCLUSIONS

In this study, the fuel flow effects in MSRs on the heat transfer and the related reactivity feedbacks are investigated. For this purpose, a numerical simulation tool was developed to model fuel flow. The effect of the number of nodes and time step on the reactor simulation results was studied and the optimum values were used in the model. Fifteen axial nodes were used for the heat transfer model and a time step of 1 ms was used in the numerical simulation. The one-dimensional time-dependent axial temperature distribution in the reactor core was used to evaluate the reactivity feedback.

The developed model was validated with the MSRE experimental results at transients. Furthermore, it was used to simulate various MSBR transients. The code showed good capability in the simulation of the reactor behavior under various transients with some deviations from the experimental results in the MSRE. This can be explained by the assumptions and simplifications in the model. Mainly, the usage of averaged heat transfer coefficients in the core without considering their change with temperature distribution.

It was observed that the change in the fuel salt temperature during the transients was limited, ensuring no salt solidification is expected. In terms of reactor stability, the negative temperature reactivity coefficient played an important role as an inherent safety characteristic in stabilizing the reactor after a transient. A comparison of the MSRE and MSBR reactor power response following transients showed the effect of strong negative reactivity feedback on the stability of the reactor. It was demonstrated that the fuel salt transit time in various primary loop components is crucial in determining the reactor dynamic response following a transient.

Even though this approach is widely used in reactor dynamics studies, an enhancement to the approach has been made by discretizing the axial fuel flow into a large number of nodes which helped in estimating the inlet and outlet fuel salt temperatures and overall reactor temperature distribution. Moreover, the developed numerical model in Visual Basic for Applications (VBA) allowed for an easier user interface and thus it can be seen as a reactor simulator. Modifications to the developed code can be implemented using a 3-dimensional heat transfer software and by considering the radial power distribution in the reactor core. In addition to that, the neutronics model can be improved by modeling the xenon behavior in the reactor.

ACKNOWLEDGMENTS

This paper is based on work supported by the project funded by the Idaho National Laboratory.

REFERENCES

1. V. Singh, A. M. Wheeler, M. R. Lish, O. Chvála, and B. R. Upadhyaya, “Nonlinear Dynamic Model of Molten-Salt Reactor Experiment – Validation and Operational Analysis,” *Annals of Nuclear Energy*, **113**, pp. 177–193 (2018).
2. E. S. Bettis, R. W. Schroeder, G. A. Cristy, H. W. Savage, R. G. Affel, and L. F. Hemphill, “The Aircraft Reactor Experiment—Design and Construction,” *Nuclear Science and Engineering*, **2**, pp. 804–825 (1957).
3. B. Prince, S. Ball, J. Engel, P. Haubenreich, and T. Kerlin, “Zero-Power Physics Experiments on the Molten-Salt Reactor Experiment (ORNL-4233),” Oak Ridge National Laboratory (1968).
4. J. Serp et al., “The molten salt reactor (MSR) in generation IV: Overview and perspectives,” *Progress in Nuclear Energy*, **77**, pp. 308–319 (2014).
5. “Molten Salt Reactor (MSR),”. https://www.gen-4.org/gif/jcms/c_9359/msr (2023).

6. P. V. Tsvetkov, *Encyclopedia of Nuclear Energy*, Management of the Nuclear Waste - Via Disposition or Transmutation, Elsevier, (2021).
7. "Application Submitted for US Molten Salt Research Reactor," https://www.world-nuclear-news.org/Articles/Application-submitted-for-US-molten-salt-research (2022).
8. International Atomic Energy Agency, *Nuclear Power Plant Instrumentation and Control: A Guidebook*, Vienna, Austria (1984).
9. H. M. Hashemian, *Nuclear Power - Control, Reliability and Human Factors*, Nuclear Power Plant Instrumentation and Control, IntechOpen, London, United Kingdom (2011).
10. J. Wang, Q. Wang, and M. Ding, "Review on Neutronic/Thermal-Hydraulic Coupling Simulation Methods for Nuclear Reactor Analysis," *Annals of Nuclear Energy*, **137** (2020).
11. M. Zarei, "Nonlinear Dynamics and Control in Molten Salt Reactors," *Nuclear Engineering and Design*, **332**, pp. 289–296 (2018).
12. J. Krepel, U. Rohde, U. Grundmann, and F. P. Weiss, "Dynamics of Molten Salt Reactors," *Nuclear Technology*, **164** (1), pp. 34–44 (2008).
13. J. Krepel, U. Grundmann, U. Rohde, and F. P. Weiss, "DYN1D-MSR Dynamics Code for Molten Salt Reactors," *Annals of Nuclear Energy*, **32**, pp. 1799–1824 (2005).
14. S. Dulla et al., "Benchmark of Dynamic Simulation Tools for Molten Salt Reactors," *Proceedings of GLOBAL 2003: Atoms for Prosperity: Updating Eisenhower's Global Vision for Nuclear Energy*, (2003).
15. R. Robertson, "Conceptual Design Study of a Single-Fluid Molten-Salt Breeder Reactor (ORNL-4511)," Oak Ridge National Laboratory (1971).
16. W. Sides, "Control Studies of A 1000-MW(e) MSBR (ORNL-TM-2927)," Oak Ridge National Laboratory (1970).
17. O. Burke, "Hybrid Computer Simulation of the MSBR (ORNL-TM-3767)," Oak Ridge National Laboratory (1972).
18. Y. Shimazu, "Nuclear Safety Analysis of a Molten Salt Breeder Reactor," *Nuclear Science and Technology*, **15** (7), pp. 514–522 (1978).
19. J. Macphee, "The Kinetics of Circulating Fuel Reactors," *Nuclear Science and Engineering*, **4**, pp. 588–597 (1958).
20. M. Zarei, "A refined Time-Delay Modeling of The Molten Salt Reactor Dynamics," *Progress in Nuclear Energy*, **117**, pp. 1–7 (2019).
21. C. Guerrieri, A. Cammi, and L. Luzzi, "An Approach to the MSR Dynamics and Stability Analysis," *Progress in Nuclear Energy*, **67**, pp. 56–73 (2013).
22. R. Robertson, "MSRE Design and Operations Report Part I" (ORNL-TM-728)," Oak Ridge National Laboratory (1965).
23. R. Steffy, P. Wood, "Theoretical Dynamic Analysis of the MSRE with 233U Fuel (ORNL-TM-2571)," Oak Ridge National Laboratory (1969).
24. S. Ball, T. Kerlin, "Stability Analysis of the Molten-Salt Reactor Experiment (ORNL-TM-1070)," Oak Ridge National Laboratory (1965).
25. B. Spinelli, "Preliminary Analysis of the MSRE Dynamic Behaviour," M.Sc. Thesis, Politecnico di Milano, Milan, Italy (2010).
26. R. Steffy, "Experimental Dynamic Analysis of The MSRE with 233U Fuel (ORNL-TM-2997)," Oak Ridge National Laboratory (1970).
27. C. Guerrieri, C. Fiorina, A. Cammi, L. Luzzi, "Preliminary Assessment of Modeling Issues Related to Dynamics and Control of Graphite-Moderated MSRs," *Proceedings of ICAPP 2011*, Nice, France, May 2-5, Paper 11099 (2011).